**Atmospheric
Measurement
Techniques
Discussions**

Column water vapor determination in night period with a lunar photometer prototype

A. Barreto[1], E. Cuevas[1], B. Damiri[2], P. M. Romero[1], and F. Almansa[1]

[1]Izaña Atmospheric Research Center, State Meteorological Agency of Spain (AEMET), Santa Cruz de Tenerife, Spain
[2]Cimel Electronique, Paris, France

Correspondence to: E. Cuevas (ecuevasa@aemet.es)

AMTD

6, 767–793, 2013

Column water vapor determination in night period

A. Barreto et al.

Title Page

Abstract	Introduction
Conclusions	References
Tables	Figures

Back | Close

Full Screen / Esc

Printer-friendly Version

Interactive Discussion

Abstract

In this paper we present the preliminary results of atmospheric column integrated water vapor (PWV) obtained with a new Lunar Cimel photometer (LC) at the high mountain Izaña Observatory in the period July–August, 2011. We have compared nocturnal PWV

5 from LC with PWV from a Global Positioning System (GPS) receiver and nighttime radiosondes (RS92). LC data have been calibrated using the Lunar Langley Method (LLM). We complemented this comparative study using quasi-simultaneous daytime PWV from Cimel AERONET (CA), GPS and RS92. Comparison of daytime PWV from CA shows differences against GPS and RS92 up to 0.18 cm. Two different filters, with

10 and approximate bandwidth of 10 nm and central wavelengths at 938 nm (Filter#1) and 937 nm (Filter#2), were mounted into the LC. Filter#1 is currently used in operational AERONET sunphotometers. PWV obtained with LC-Filter#1 showed an overestimation above 0.18 and 0.25 cm compared to GPS and RS92, respectively, meanwhile Filter#2, with a reduced out-of-band radiation, showed very low differences compared with the

15 same references (≤ 0.03 cm).

These results demonstrate the ability of the new lunar photometer to obtain accurate and continuous PWV measurements at night in addition to the notably influence of the filter's transmissivity response on PWV determination at nighttime. The use of enhanced bandpass filters in lunar photometry, which is affected by more important in-

20 accuracies than sun-photometry, is necessary to infer PWV with similar precision than AERONET.

1 Introduction

Precipitable water vapor (PWV) is the total atmospheric water vapor contained in a vertical column of unit cross-sectional area extending between any two specified levels.

25 In this work we will refer PWV as the column integrated water vapor contained in a

column of a unit cross-section extended all the way up from the earth's surface to the top of the atmosphere.

Water vapor is the most important atmospheric greenhouse gas, and its phase's changes involve exchanges of latent heat energy affecting the vertical stability of the atmosphere, the evolution of the weather and the energy balance of the global climate system (Chanine, 1992). There are indications that the amount of PWV is changing but a very low rate, few tenths of mm per decade (Trenberth et al., 2005; Wagner et al., 2006), so a high quality worldwide long-term PWV monitoring is essential. PWV is currently observed by a number of sensors onboard satellite platforms, as the Moderate Resolution Imaging Spectroradiometer (MODIS) on Terra and Aqua platforms (Kaufman and Gao, 1992), the Atmospheric Infrared Sounder (AIRS) onboard Aqua (Bedka et al., 2010) or the Infrared Atmospheric Sounding Interferometer (IASI) onboard the EUMESAT polar satellite MetOp (Pougatchev et al., 2009). Satellite borne observations have the advantage to obtain a global picture of PWV distribution on a daily basis, although with poor temporal resolution and point discrimination, and relatively high uncertainties associated with long term monitoring due to the lack of sensor stability in time. These observations are complemented with ground-based remote sensing techniques, such as Global Positioning System (GPS), thermodynamic radiosondes (e.g. RS92) or sun-photometry (e.g. Cimel/AErosol RObotic NETwork – AERONET – sunphotometers). GPS uses the delay in radio signals due to the permanent dipole moment of water vapor molecules in the atmosphere to infer PWV (Duan et al., 1996), and Vaisala RS92 radiosonde technique obtains direct measurement of water vapor as a function of height by means of a capacitance relative-humidity sensor (Miloshevich et al., 2009). Sun-photometry measures atmospheric transmission of solar radiation within the 940-nm water vapor absorption band, and then obtain a column-averaged value of water abundance (Halthore et al., 1997). PWV can also be measured by means of other instruments, such as Raman Lidars or microwave radiometers (Schmid et al., 2001).

A. Barreto et al.

The ground-based remote sensing techniques are especially valuable for validating satellite PWV (Alexandrov et al., 2009) and for improving the temporal resolution and simplicity of PWV determination (Halthore et al., 1997). However, GPS technique shows poor precision ($\sim 20\%$) at low PWV conditions (< 3.5 mm) (Schneider et al.,
5 2010), so that this technique has significant limitations in dry regions, such as the subtropics and the poles. Raman Lidars and microwave radiometers are complex and expensive instruments to set up a global network. Radiosondes routine operation is also rather expensive and for this reason they are flown normally only twice a day (00:00 and 12:00 UTC) in a limited number of stations worldwide. PWV from radiosondes is
10 basically obtained with integrated water vapor measured from ground to the upper troposphere. Miloshevich et al. (2009) estimated a precision $\sim 5\%$ in PWV derived using RS92 once an empirical correction procedure to remove the mean bias error in this instrument was implemented. In the upper troposphere and for very dry conditions the precision of the PWV inferred using this technique is ~ 10–20% (Schneider et al.,
15 2010). Holben et al. (2001) estimated a precision in PWV from sun-photometry $\sim 10\%$ as a result of the method for PWV retrieval and the relatively large uncertainty in the V_0 determined using the Langley Method in ~ 940 nm channel.

Due to the high temporal resolution and simplicity of sunphotometers, as well as the capacity of providing a quasi-continuous PWV information, this technique is widely
20 used. Unfortunately, it is restricted to the light period. Thus, it becomes an important limitation for a continuous PWV monitoring when strong variations are observed between day and night, in polar regions or in high mountain stations, in which background values, normally representative of free troposphere conditions during catabatic regime, are mostly present during the night. The unavailability of PWV data in periods of darkness
25 ness is a real handicap to this technique.

In this study we have complemented the nocturnal aerosol optical depth study performed by Barreto et al. (2012) using a new lunar photometer prototype (*Cimel Electronique* CE-318U) with an analysis of PWV at night. Barreto et al. (2012) developed a new methodology to calibrate nocturnal photometers which can solve the problem of

moon's illumination variation during the course of the night, the Lunar Langley Method (LLM).

This paper is organized as follows. The site of measurements is briefly described in Sect. 2. The main features of the new lunar photometer, as well as the ancillary information used for PWV validation, are shown in Sect. 3. In Sect. 4 we describe the methodology to obtain PWV with a lunar photometer. In Sect. 5 we analyze and compare nocturnal PWV obtained with a lunar photometer, using two different filters centered near 940 nm, with coincident nocturnal data from GPS and RS92. In addition, we compare quasi-simultaneous daylight PWV obtained from AERONET, GPS and RS92. Finally, in Sect. 6 the discussion and the main conclusions are presented.

2 Site information

Izaña Observatory (IZO; www.aemet.izana.org) is a high mountain Global Atmospheric Watch (GAW) station located in Tenerife (the Canary Islands, Spain) at $28°18'$ N , $16°29'$ W and 2373 m a.s.l. It is part of the Izaña Atmospheric Research Centre (IARC), managed by the State Meteorological Agency of Spain (AEMET). IZO is normally above the level of a strong and persistent subsidence temperature inversion that prevents pollution from the lower part of the island. The site is characterized by pristine skies, a high atmospheric stability, low and stable total column O_3, and very low atmospheric humidity, resulting a suitable site for background monitoring, representative of free troposphere conditions. These background conditions are reinforced during night period when a strong catabatic regime is well established. Radiation, in-situ trace gases and aerosols, as well meteorological parameters, are continuously monitored within GAW. NDACC (Network for the Detection of Atmospheric Composition Change) FTIR (Fourier Transform Infrared), DOAS/UV-VIS, UV-Brewer and O3-ECC programmes are held for many years at IZO. RS92 soundings are launched twice a day (00:00 and 12:00 UTC) from the Güímar station ($28°32'$ N , $16°38'$ W , 105 m a.s.l.), near the coast, approximately 15 km to the south of IZO.

3 Instrumentation

3.1 The new Lunar Cimel CE-318U

The new Lunar Cimel CE-318U photometer (hereafter referred as LC) is extensively described in Barreto et al. (2012). LC is in essence a quite similar instrument to the usual CE-318 sunphotometer of AERONET (Holben et al., 1998), but with some significant technical modifications to optimize its performance for moon observations.

LC performs direct measurements at eight nominal wavelengths: 1640, 1020, 938, 937, 870, 675, 500 and 440 nm. The LC has been equipped with two band filters centered within water vapor absorption band, with an approximate Full Width at Half Maximum (FWHM) of 10 nm, approximately centered at 940 nm. This feature constitutes an interesting opportunity for investigating the PWV obtained with different interference filters. The two filters present the maximum transmissivity set at the central wavelength of 937 and 938 nm, respectively.

Filter#1, centered at 938 nm, is the current band filter used by the AERONET CE-318 sunphotometers. It presents a transmissivity up to 0.7 and an important contribution of wavelengths outside the FWHM (Fig. 1). Out-of-band values are called "wings of the filter". However, Filter#2 is characterized by flat shape transmissivity close to 1 at central wavelength of 937 nm with negligible out-of-band radiation effect. Previous studies developed by Halthore et al. (1997) pointed out that water abundance is not sensitive to the position of the filter within the absorption band. These authors estimated the error due to this effect to values typically $< 1\%$, pointing to the filter bandwidth as the principal source of error, apart from the instrument calibration errors. However, the importance of using different narrowband filter responses was not clearly established in this study. Ortiz de Galisteo et al. (2009) showed the importance of the "wings of the filter" effect, which might introduce an overestimation in the aerosol optical depth, and thus inaccuracies in PWV retrieval due to uncertainties on Rayleigh and gaseous absorption total optical depth. This problem was also studied by Alexandrov et al. (2009). These authors estimated that background transmittances from 10^{-4} to 10^{-7} needed to

be blocked. Furthermore, they showed that a background transmittance $\sim 10^{-4}$ lead to an error in aerosol optical depth up to 10 % and appreciably variations in "a" and "b" parameters in the T_w-PWV exponential dependence presented in Bruegge et al. (1992).

5   In the present study we have compared PWV obtained with the two LC filters with markedly different transmission responses. To do this, we have performed direct moon measurements in the periods from 11 to 15 July 2011, and from 9 to 16 August 2011.

3.2 Ancillary information for PWV validation

AERONET Version 2 Level 1.5 data was obtained using the Izaña AERONET Mas-
10 ter Cimel #244 (http://aeronet.gsfc.nasa.gov), hereafter refered as AC, for days before and after each nocturnal LC observation. PWV was measured from direct sun mea-surements in the ~ 940 nm channel. They are automatically cloud screened using the methodology proposed by Smirnov et al. (2000). Following Holben et al. (2001), due to the uncertainties involved in extracting PWV from the water vapor transmittance ($T_{\mathrm{w},\lambda}$)
15 and the relatively large uncertainty (between 2–4 %) in the modified Langley V_0 as a re-sult of water vapor variability, an estimated uncertainty of ±10 % is expected for PWV derived from sun-photometry.

    The radio signals of GPS and GLONASS (the Russian GPS) are delayed due to re-fraction in the atmosphere, mainly caused by water vapor. The Zenith Total Delay (ZTD)
20 is the sum of the Zenith Hydrostatic Delay (ZHD), associated with induced dipole mo-ments of the atmospheric molecules (the dry component), and the Zenith Wet Delay (ZWD) related to the permanent dipole moments of the water vapour molecules (Duan et al., 1996). A Leica GRX 1200GG pro GPS/GLONASS receiver has been operated at IZO within the European Reference Frame network (EUREF, Bruyninx, 2004) since July
25 2008. This instrument belongs to the Spanish National Geographical Institute (IGN), which provides 15-min instantaneous ZTD values calculated by applying the Bernese software (Rothacher, 1992, 1993). The ZHD is calculated at IZO with the actual surface

pressure at the station which is measured with a high-precision SETRA 470 barometer. The ZHD is typically one order of magnitude larger than the ZWD. The ZWD is then converted to PWV using the refraction constants of water vapour ("map function") derived from column averaged temperature obtained from radiosondes. This method is described by Romero et al. (2009). The Izaña's GPS/GLONASS receiver is part of the EUMETNET (the Network of European Meteorological Services) GPS water vapour programme (E-GVAP). According to Schneider et al. (2010), the GPS technique has a detection limit in column water vapor of 3.5 mm, and below this threshold the GPS systematically underestimates the PWV. Above 3.5 mm, the GPS accuracy is better than 10 %, an estimated error of 0.7 mm, and a small bias with respect to FTIR data is observed (Schneider et al., 2010).

Vaisala RS92 radiosonde water vapor measurements have been included in this comparison. Meteorological radiosondes have been launched twice a day (00:00 and 12:00 UTC) from a radiosonde station (Güímar-Tenerife) situated at the coastline, approximately 15 km to the south of Izaña. Güímar radiosonde WMO station #60018 is part of Global Climate Observing System (GCOS)-Upper-Air Network (GUAN). The RS92 sonde performs relative humidity measurements as a function of height using a thin-film capacitance which is proportional to the ambient water vapor concentration (Miloshevich et al., 2009). Data has been corrected by temperature and radiation dependence (in the case of daytime soundings) following Romero et al. (2011). The estimated precision is 5 % for total column water vapor in the lower and middle troposphere, although the precision is significantly lower (about 10–20 %) in the upper troposphere and for very dry conditions (Miloshevich et al., 2009; Schneider et al., 2010). Schneider et al. (2010) estimated a RS92's PWV precision of 15 % by comparison with FTIR, being this precision independent of atmospheric conditions.

Column water vapor determination in night period

A. Barreto et al.

Title Page

Abstract | Introduction

Conclusions | References

Tables | Figures

|◄ | ►|

◄ | ►

Back | Close

Full Screen / Esc

Printer-friendly Version

Interactive Discussion

4 Methodology

The Beer-Lambert-Bouguer Law can be applied over small band passes characterized by reduced spectral variation in atmospheric transmittance (Schmid et al., 1996). In those regions affected by strong spectral variation of molecular absorption, as occurred in near-infrared water vapor absorption band, this law must be modified taking into account the water vapor transmittance ($T_{w,\lambda}$),

$$V(\lambda) = V_{0,\lambda} \cdot \exp(-m(\theta) \cdot \tau_\lambda) \cdot T_{w,\lambda}. \tag{1}$$

V_λ is the output voltage, $V_{0,\lambda}$ represents the extraterrestrial voltage, m is the atmospheric air mass, θ the moon's zenith angle and τ_λ is the spectral optical depth. Neglecting the absorption due to O_3 and NO_2 in this spectral range, only the contribution of water vapor, Rayleigh and aerosols are considered in Eq. (1), and thus,

$$V_\lambda = V_{0,\lambda} \cdot \exp(-m_R(\theta) \cdot \tau_{R,\lambda} - m_a(\theta) \cdot \tau_{a,\lambda}) \cdot T_{w,\lambda}. \tag{2}$$

τ_R and τ_a represent the Rayleigh and aerosol optical depths, respectively, meanwhile m_R and m_a are the Rayleigh and aerosol air masses. $T_{w,\lambda}$ can be defined as the band weighted water vapor transmittance (Thomason, 1985),

$$T_{w,\lambda} = \frac{\int_{\lambda_1}^{\lambda_2} E_0(\lambda) \cdot S(\lambda) \cdot \exp(-m_w \cdot \tau_w(\lambda)) d\lambda}{\int_{\lambda_1}^{\lambda_2} E_0(\lambda) \cdot S(\lambda) d\lambda} \tag{3}$$

where $\tau_{w,\lambda}$ is the strongly varying water vapor absorption optical depth, $E_0(\lambda)$ is the exo-atmospheric solar irradiance and $S(\lambda)$ represents the instrument response in each channel. The parameter m_w represents the water vapor optical air mass. The dependence of $T_{w,\lambda}$ on the PWV was studied by Bruegge et al. (1992), showing the following exponential dependence,

$$T_{w,\lambda} = \exp(-a \cdot (m_w(\theta) \cdot PWV)^b). \tag{4}$$

In this equation, "a" and "b" constants can be determined by fitting the weighted water vapor transmittances simulated by a radiative transfer model for an instrument specific filter function. Thus, a fitting plot of $\ln(\ln(\frac{1}{T_w}))$ against $\ln(m_w \cdot \mathrm{PWV})$ results in a line with a slope equal to "b", and an intercept of $\ln(a)$. As Halthore et al. (1997) showed, these

5 constants depends on wavelength position, the width and shape of the photometer filter functions, the atmospheric pressure and temperature as well as the vertical distribution of water vapor. In this study we have used the radiative code MODTRAN 4.0 to estimate water vapor transmittances. In order to account for nocturnal humidity conditions, 153 vertical soundings launched at 00:00 UTC from the AEMET Güímar station have been

10 introduced in the radiative code. A variation of θ between 0 and 80° in each profile has been considered to introduce PWV variation. Combining Eqs. (2) and (4), PWV can be determined using the following equation:

$$\mathrm{PWV} = \frac{1}{m_w} \cdot \left\{ \frac{1}{a} \cdot \left[\ln\left(\frac{V_{0,\lambda}}{V_\lambda} \right) - m_R \cdot \tau_{R_\lambda} - m_a \cdot \tau_{a,\lambda} \right] \right\}^{\frac{1}{b}} . \tag{5}$$

15 V_0 is obtained in sun-photometry by means of the Langley-plot method once τ_a within the $\sim 940\,\mathrm{nm}$ water vapor absorption band is estimated by extrapolation of $\tau_{a,\lambda}$ at 870 and 440 nm. In case of lunar photometry, Barreto et al. (2012) developed the LLM as a calibration method to account for the moon's illumination variations inherent to the lunar cycle. This new methodology is suitable to calibrate nocturnal photometers under

20 changeful illumination conditions. These authors found similar nocturnal τ_a uncertainties using this method than those associated to the usual solar Langleys, i. e. ±0.02 for 500 and 440 nm channels, and ±0.01 for longer wavelengths channels. This method considers the extraterrestrial voltage as,

25 $$V_{0,\lambda} = I_{0,\lambda} \cdot \kappa_\lambda . \tag{6}$$

The spectral calibration coefficients (κ_λ) in this equation depend on the instrument's features (Barreto et al., 2012). $I_{0,\lambda}$ is the extraterrestrial irradiance estimated from the

A. Barreto et al.

lunar irradiance model presented in Kieffer and Stone (2005). This empirical model, known as ROLO (RObotic Lunar Observatory), estimates the exoatmospheric lunar irradiance using a telescope system with the capability to perform measurement at 32 different VNIR and SWIR passbands. However, a continuum lunar irradiance spectrum was obtained from a smoothing analysis of the discrete ROLO irradiances, and therefore $I_{0,\lambda}$ for each LC bands were obtained by convolving spectral irradiances with filter response functions. The orbital parameters required as ROLO inputs were computed using the astronomical calculator Alcyone 4.0.

Following Barreto et al. (2012), the instrument calibration was performed using lunar data obtained on 8–9 February 2012. This night was selected due to the relatively low and constant aerosol concentration, especially during the moonset, when the aerosol optical depth at 440 nm remained stable and near 0.02. The κ_λ's for each channel are presented in Table 1.

Once the calibration coefficients have been calculated, τ_a for Filters #1 and #2 are retrieved by extrapolation of 870 and 440 nm values. Then, both calibration coefficients in the water vapor absorption band (κ_{wv}'s) are calculated using a fitting plot, and PWV can be obtained as follows,

$$\text{PWV} = \frac{1}{m_w} \cdot \left\{ \frac{1}{a} \cdot \left[\ln\left(\frac{I_{0,wv}}{V_{wv}}\right) + \ln(\kappa_{wv}) - m_R \cdot \tau_{R,wv} - m_a \cdot \tau_{a,wv} \right] \right\}^{\frac{1}{b}} . \tag{7}$$

Due to the high spatial and temporal variability of the atmospheric water vapor, it is particularly important to establish an adequate coincidence criterion for comparing PWV measurements from different techniques. Since GPS provides PWV data every 15 min, we have considered quasi-simultaneous LC-GPS and CA-GPS measurements when they overlap within the time interval of ±6 min. Regarding comparisons against RS92 PWV data, as we have only two values per day (around 00:00 and 12:00 UTC), we have compared LC-RS92 PWV within the 22:00–0:00 UTC time period, and CA-RS92 PWV within 10:00–12:00 UTC.

5   Results

Following the exponential dependence of T_w with respect to PWV presented in Eq. (4), we have calculated the filter dependent constants ("a" and "b"). Values of "a" and "b" for the two LC water vapor bands are given in Table 2. The correlation coefficient R of the fitting plot is 0.99 for the two filters. We can see that "b" coefficients are similar for both filters, while "a" coefficients are appreciably different. As "a" represents the intercept of the T_w-PWV fitting line, this result points out the impact of the filter function shape on the PWV retrieval. The lower "a" coefficient found for Filter#1 is due to the overestimation of T_w as a result of the out-of-band radiation effect.

The comparison of GPS/AC pairs and GPS/LC pairs for both filters centered at 937 nm and 938 nm using the LLM for 11–15 July and 9–16 August are presented in Figs. 2 and 3, respectively. The comparison during daytime has been performed with 112 pairs for July and 104 for August, respectively. The correlation coefficients (R) are 0.97 for July and 0.92 for August. GPS and LC data have been compared using 81 pairs in July and 103 in August. Correlation coefficients are similar to those obtained in daytime (0.90 and 0.98 in July and August for filters #1 and #2, respectively).

PWV differences between sun/moon photometers versus GPS and RS92 are quantified in Tables 3 and 4, where the mean value, the standard deviation (σ) and the root-mean-square-error (RMSE) are presented. In Figs. 4 and 5 the daily PWV evolution for LC, CA, GPS and RS92 in July and August cases, respectively, are displayed jointly with the vertical water vapor partial pressure cross-sections from the radiosonde (upper panel). In these figures daytime information corresponds to PWV extracted approximately at 11:00 UTC and nighttime to data about 23:00 UTC. From Table 3 we obtained a significant low bias (< 0.02 cm) in the comparison between LC-Filter#2 and GPS for July, similar to those found for GPS/CA (-0.01 cm). Table 4 shows that the best scores for RS92 and sun/moon photometer comparison in July were obtained for RS92/LC-Filter#2 (0.03 cm), with the lowest differences, standard deviation and RMSE. These values are within the estimated PWV precision for both techniques

Title Page

Abstract | Introduction

Conclusions | References

Tables | Figures

|◄ | ►|

◄ | ►

Back | Close

Full Screen / Esc

Printer-friendly Version

Interactive Discussion

(Holben et al., 2001; Schneider et al., 2010). However, higher discrepancies were obtained when comparing GPS and LC-Filter#1 ($\sim$ 0.18 cm), RS92 and CA (-0.14 cm) and RS92 and LC-Filter#1 (0.26 cm). There is a good agreement between GPS/LC-Filter#2, GPS/CA as well as RS92/LC-Filter#2 (Fig. 4), in spite the relatively high PWV difference GPS/CA found for 11 July. It is probably due to the fact that PWV was below the GPS detection limit (0.35 cm). This dry period was well depicted by the vertical water vapor partial pressure cross-section of the radiosonde. It was followed by a notable increase of atmospheric humidity in levels lower than 3 km height, especially during 12 and 13 July. During 12 July at nighttime relatively high PWV values ($\sim$ 1 cm) were recorded by LC-Filter#2, GPS and RS92. PWV from by LC-Filter#1 reached to 1.2 cm. Daytime RS92 data on 13 July presented similar PWV values than the previous night, while PWV extracted by GPS and CA were considerably lower (< 0.6 cm). According to radiosonde data, the atmospheric humidity remained high and nearly constant during 12 to 13 July, decreasing and being restricted to lower levels from 14 July. This reduction was more pronounced from the last part of 14 July on. It was well captured by LC-Filter#2.

In relation to August data, similar PWV differences were shown in Tables 3 and 4 for GPS/CA (-0.16 cm), RS92/CA (-0.18 cm) and GPS/LC-Filter#1 (0.19 cm), meanwhile more pronounced discrepancies up to 0.25 cm were obtained in the RS92/LC-Filter#1 comparison. These results are in contrast to differences up to 0.02 cm when PWV from GPS/LC-Filter#2 and RS92/LC-Filter#2 were compared. Figure 5 shows a lower temporal variability in PWV during August than it was displayed in July, when only a few increases in PWV occurred. This PWV evolution is well tracked by GPS and LC-Filter#2. PWV decreased from daytime to nighttime period in 9 August and it continued decreasing until 10 August at night, when a good agreement between GPS, RS92 and LC-Filter#2 was found. GPS and CA PWV in 11 August were quite similar, meanwhile RS92 detected PWV values near 1 cm. Nighttime data presents again a good concordance between RS92 and LC-Filter#2. Lower and more stable PWV values were expected for the next two days period, as those displayed by CA, LC-Filter#2 and RS92.

After this period, the atmospheric humidity experienced a notable increase, reaching values > 1 cm in 15 August. Lower values were retrieved by CA.

6 Summary and conclusions

The preliminary results of nocturnal PWV performed in this study demonstrate that LC-Filter#1 and Filter#2 correlate quite well to PWV from GPS. These regressions were similar to those obtained by means of diurnal CA data. LC-Filter#2 and GPS absolute PWV differences in July and August were very low (0.01 cm), as well as between AC and GPS differences in July at daytime (0.01 cm). Oppositely, CA underestimated notably PWV from GPS in August cases (0.16 cm) and an overestimation of GPS ~ 0.19 cm was found for LC-Filter#1 at nighttime. The comparative study between Cimel daytime and nighttime PWV with RS92 information showed again a good concordance in case of LC-Filter#2, with differences ≤ 0.03 cm. However, LC-Filter#1 absolute differences were notably higher, up to 0.26 cm, as well as diurnal differences (~ 0.18 cm), above the instrument's expected precision. These quantitative results were confirmed by a qualitatively study of the daily PWV evolution within the period of study. We have found that LC-Filter#2 and RS92 present a pretty good agreement, providing notably similar values during the whole period. Reasonable PWV daily differences in relation to GPS data were also obtained, being within the accuracy expected for these instruments (Schneider et al., 2010).

Finally, it is important to highlight the systematic differences in PWV obtained for both LC filters. Since the central wavelengths of these channels differ in approximately 1 nm and they have a similar FWHM, it proves that water vapor data inferred by filter radiometry is very sensitive to filter's shape. Although the filter transmission inside the LC-Filter#1 wings is very low, the relatively strong transmission of water vapor in this spectral range supposes a significant contribution that must be taken into account. The radiation transmitted by Filter#1 outside the FWHM, or out-of-band radiation, lead us to "*a*" and "*b*" values lower than expected and therefore errors in the spectral calibration

coefficients (κ_{wv}) in this spectral range. On the contrary, the contribution of out-of-band radiation in Filter#2 can be negligible, and thus a more accurate PWV determination can be carried out using this filter, as our results showed. Thus, we have confirmed that in case we have information from a filter with a relatively high contribution in the wings

5   it is necessary to block the out-of-band radiation.

To conclude, this paper proves the ability of the new CE-318U Lunar Cimel to perform accurate nocturnal column water vapor measurements, comparable to the accuracy of other similar techniques. It could be of considerable importance to fill the gaps in PWV inferred using sun-photometry as well as to provide a continuous sequence of

10   PWV measurements at night. In addition, the use of improved interference filters with higher transmission responses are proven to reduce considerably the inaccuracies in PWV determination at nighttime. Since lunar photometry is affected by more important inaccuracies than sun-photometry, the use of enhanced bandpass filters is essential to obtain accurate PWV with a precision similar to that of the AC.

References

Alexandrov, M. D., Schmid, B., Turner, D. D., Cairns, B., Oinas, V., Lacis, A. A., Gutman, S. I., Westwater, E. R., Smirnov, A., and Eilers, J.: Columnar water vapor retrievals from multifilter rotating shadowband radiometer data, J. Geophys. Res., 114, D02306, doi:10.1029/2008JD010543, 2009. 770, 772

Barreto, A., Cuevas, E., Damiri, B., Guirado, C., Berkoff, T., Berjón, A. J., Hernández, Y., Almansa, F., and Gil, M.: A new method for nocturnal aerosol measurements with a lunar photometer prototype, Atmos. Meas. Tech. Discuss., 5, 5527–5569, doi:10.5194/amtd-5-5527-2012, 2012. 770, 772, 776, 777

Bedka, S., Knuteson, R., Revercomb, H., Tobin, D., and Turner, D.: An assessment of the absolute accuracy of the Atmospheric Infrared Sounder v5 precipitable water vapor product at tropical, midlatitude, and arctic ground-truth sites: September 2002 through August 2008, J. Geophys. Res., 115, D17310, doi:10.1029/2009JD013139, 2010. 769

Bruegge, C. J., Conel, J. E., Green, R. O., Margolis, J. S., Holm, R. G., and Toon, G.: Water vapor column abundances retrievals during FIFE, J. Geophys. Res., 97, 18759–18768, 1992. 773, 775

Chahine, M. T.: The hydrological cycle and its influence on climate, Nature, 359, 373–380, 1992. 769

Duan, J., Bevis, M., Fang, P., Bock, Y., Chiswell, S., Businger, S., Rocken, C., Solheim, F., van Hove, T., Ware, R., McClusky, S., Herring, T. A., and King, R. W.: GPS meteorology: direct estimation of the absolute value of precipitable water, J. Appl. Meteorol., 35, 830–838, 1996. 769, 773

Halthore, R. N., Eck, T. F., Holben, B. N., and Markham, B. L.: Sun photometric measurements of atmospheric water vapor column abundance in the 940-nm band, J. Geophys. Res., 102, 4343–4352, 1997. 769, 770, 772, 776

Holben, B. N., Eck, T. F., Slutsker, I., Tanré, D., Buis, J. P., Setzer, A., Vermote, E., Reagan, J. A., Kaufman, Y. J., Nakajima, T., Lavenu, F., Jankowiak, I., and Smirnov, A.: AERONET – a federated instrument network and data archive for aerosol characterization, Remote Sens. Environ., 66, 1–16, 1998. 772

Holben, B. N., Tanre, D., Smirnov, A., Eck, T. F., Slutsker, I., Abuhassan, N., Newcomb, W. W., Schafer, J. S., Chatenet, B., Lavenu, F., Kaufman, Y. J., Vande Castle, J., Setzer, A., Markham, B., Clark, D., Frouin, R., Halthore, R., Karneli, A., O'Neill, N. T., Pietras, C., Pinker, R. T., Voss, K., and Zibordi, G.: An emerging ground-based aerosol climatology: aerosol optical depth from AERONET, J. Geophys. Res., 106, 12067–12097, 2001. 770, 773, 779

Kaufman, Y. J. and Gao, B. C.: Remote sensing of water vapor in the near IR from EOS/MODIS, IEEE T. Geosci. Remote, 30, 871–884, 1992. 769

Kieffer, H. H. and Stone, T. C.: The spectral irradiance of the moon, Astron. J., 129, 2887–2901, 2005. 777

Miloshevich, L. M., Vömel, H., Whiteman, D. N., and Leblanc, T.: Accuracy assessment and correction of Vaisala RS92 radiosonde water vapor measurements, J. Geophys. Res.-Atmos., 114, D11305, doi:10.1029/2008JD011565, 2009. 769, 770, 774

Ortiz de Galisteo, J. P., Cachorro, V. E., Toledano, C., Rodríguez, E., Berjón, A., and de Frutos, A. M.: Error source in AOD retrieval from filter radiometer data in the UV due to filter band function, Aerosol Sci., 40, 597–602, 2009. 772

Pougatchev, N., August, T., Calbet, X., Hultberg, T., Oduleye, O., Schlüssel, P., Stiller, B., Germain, K. St., and Bingham, G.: IASI temperature and water vapor retrievals – error assessment and validation, Atmos. Chem. Phys., 9, 6453–6458, doi:10.5194/acp-9-6453-2009, 2009. 769

Romero, P. M., Cuevas, E., Ramos, R., Valdés, M., and Schneider, M.: Programa de vapor de agua en columna del Centro de Investigación Atmosférica de Izaña: análisis e intercomparación de diferentes técnicas de medida, NIPO: 784-09-009-9, Agencia Estatal de Meteorología, Ministerio de Medio Ambiente, y Medio Rural y Marino, Madrid, Spain, 2009. 774

Romero, P. M., Marrero de la Santa Cruz, C. L., Alonso, S., Cuevas, E., Afonso, S., and Ortiz de Galisteo, J. P.: Una climatología de agua precipitable en la región subtropical sobre la isla de Tenerife basada en datos de radiosondeo, NIPO: 281-12-007-5, Agencia Estatal de Meteorología, Ministerio de Medio Ambiente, y Medio Rural y Marino, Madrid, Spain, 2011. 774

Rothacher, M.: Orbits of Satellite Systems in Space Geodesy, Geodätisch-geophysikalische Arbeiten in der Schweiz, Band 46, Schweizerische Geodätische Kommission, Institut für Geodäsie und Photogrammetrie, Eidg. Technische Hochschule Zurich, Zurich, 1992. 773

Rothacher, M., Beutler, G., Gurtner, W., Brockmann, E., and Mervart, L.: The Bernese GPS Software Version 3.4, Druckerei der Universität Bern, Astronomical Institute, University of Berne, 1993. 773

Schmid, B., Thome, K. J., Demoulin, P., Peter, R., Mätzler, C., and Sekler, J.: Comparison of modeled and empirical approaches for retrieving columnar water vapor from solar transmittance measurements in the 0.94-μm region, J. Geophys. Res., 101, 9345–9358, 1996. 775

Schmid, B., Michalsky, J. J., Slater, D. W., Barnard, J. C., Halthore, R. N., Liljegren, J. C., Holben, B. N., Eck, T. F., Livingston, J. M., Philip, Russell, B., Ingold, T., and Slutsker, I.: Comparison of columnar water-vapor measurements from solar transmittance methods, Appl. Optics, 40, 1886–1896, 2001. 769

Schneider, M., Romero, P. M., Hase, F., Blumenstock, T., Cuevas, E., and Ramos, R.: Continuous quality assessment of atmospheric water vapour measurement techniques: FTIR, Cimel, MFRSR, GPS, and Vaisala RS92, Atmos. Meas. Tech., 3, 323–338, doi:10.5194/amt-3-323-2010, 2010. 770, 774, 779, 780

Smirnov, A., Holben, B. N., Eck, T. F., Dubovick, O., and Slutsker, I.: Cloud screening and quality control algorithms for the AERONET database, Remote Sens. Environ., 73, 337–349, 2000. 773

Trenberth, K. E., Fasullo, J., and Smith, L.: Trends and variability in column-integrated atmospheric water vapour, Clim. Dynam., 24, 741–758, 2005. 769

Wagner, T., Beirle, S., Grzegorski, M., and Platt, U.: Global trends (1996–2003) of total column precipitable water observed by Global Ozone Monitoring Experiment (GOME) on ERS-2 and their relation to near-surface temperature, J. Geophys. Res., 111, D12102, doi:10.1029/2005JD006523, 2006. 769

Table 1. κ_j calibration coefficients ($W^{-1} m^2 nm\,DC$) extracted for each LC channel obtained during the moonset of 9 February 2012.

Channel	1020	1640	938	937	870	675	500	440
κ_j	2.15×10^9	1.28×10^{10}	3.36×10^9	3.37×10^9	3.02×10^9	2.29×10^9	1.74×10^9	1.41×10^9

Table 2. Coefficients a and b obtained for Filter#1 centered at 938 nm and Filter#2 at 937 nm.

	Filter#1	Filter#2
a	0.5145	0.5929
b	0.5607	0.5777

Table 3. Mean, standard deviation σ and RMSE (cm) of the PWV difference (photometer minus GPS data) obtained from the comparison study between diurnal CA, nocturnal LC and GPS.

		GPS	
		July	August
AERONET Cimel	Mean and σ	-0.01 ± 0.13	-0.16 ± 0.11
	RMSE	0.13	0.18
Lunar Cimel (Filter#1)	Mean and σ	0.18 ± 0.18	0.19 ± 0.10
	RMSE	0.25	0.24
Lunar Cimel (Filter#2)	Mean and σ	-0.01 ± 0.14	-0.01 ± 0.11
	RMSE	0.19	0.11

Column water vapor determination in night period

A. Barreto et al.

Table 4. Mean, standard deviation σ and RMSE (cm) of the PWV difference (photometer minus RS92 data) obtained from the comparison study between diurnal CA, nocturnal LC and RS92 data.

		RS92	
		July	August
AERONET Cimel	Mean and σ	-0.14 ± 0.15	-0.18 ± 0.12
	RMSE	0.21	0.21
Lunar Cimel (Filter#1)	Mean and σ	0.26 ± 0.04	0.25 ± 0.07
	RMSE	0.19	0.24
Lunar Cimel (Filter#2)	Mean and σ	0.03 ± 0.02	0.02 ± 0.10
	RMSE	0.03	0.10

Column water vapor determination in night period

A. Barreto et al.

Fig. 1. Filter transmission responses associated to both LC channels located within water vapor absorption band. MODTRAN Mid-latitude summer water vapor transmission is also included.
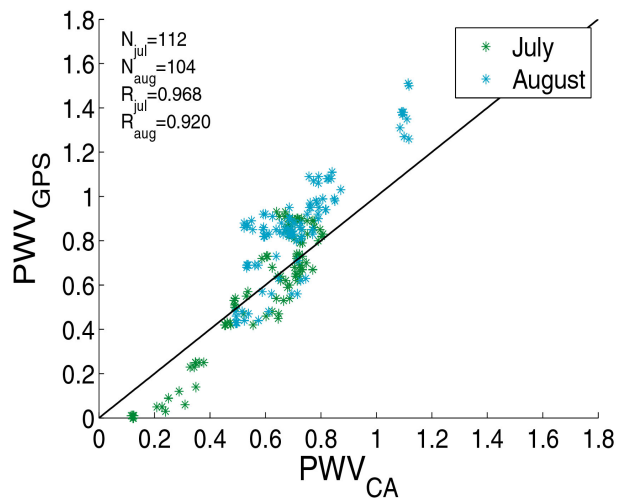
Fig. 2. Correlation between PWV (cm) obtained by means of GPS and CA database. The number of pairs as well as the correlation coefficient (R) for each month have been included.

Full Screen / Esc

Printer-friendly Version

Interactive Discussion
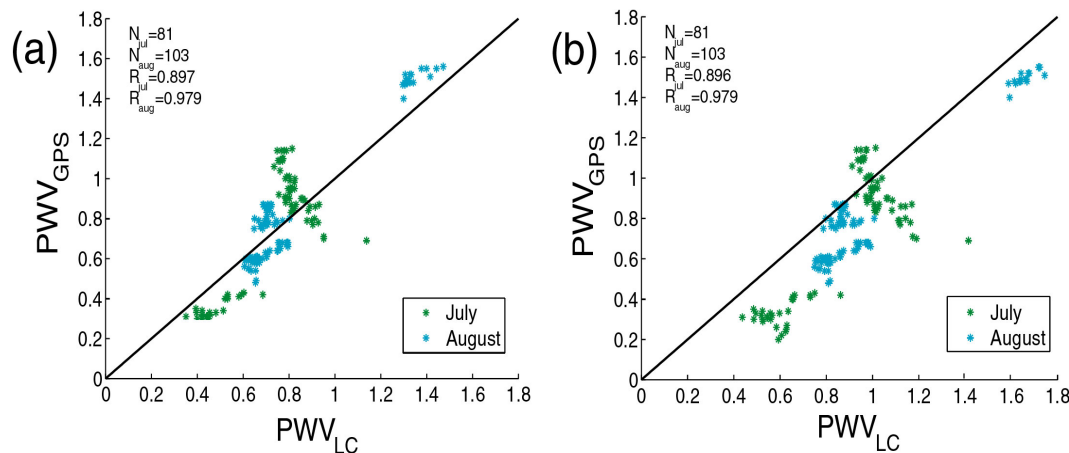
Fig. 3. PWV-GPS (cm) versus PWV-LC (cm) for channels centered at **(a)** 937 nm and **(b)** 938 nm. The number of pairs as well as the correlation coefficient (R) for each month have been included.
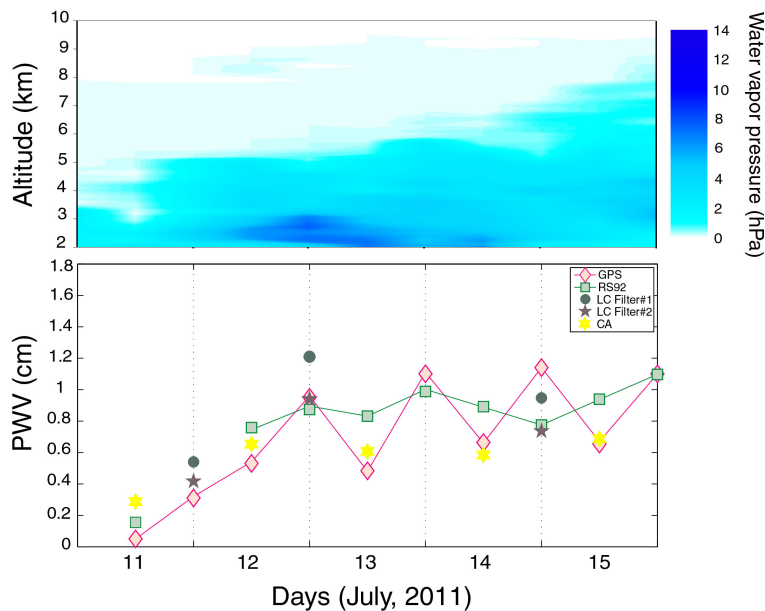
Fig. 4. Daily evolution of PWV (cm) obtained in July at daytime ($\sim$11:00 UTC) and nighttime ($\sim$23:00 UTC) using CA and LC, as well as GPS and RS92. In the upper panel is presented the vertical daily evolution of water vapor pressure (hPa) during this period obtained from radiosonde data.
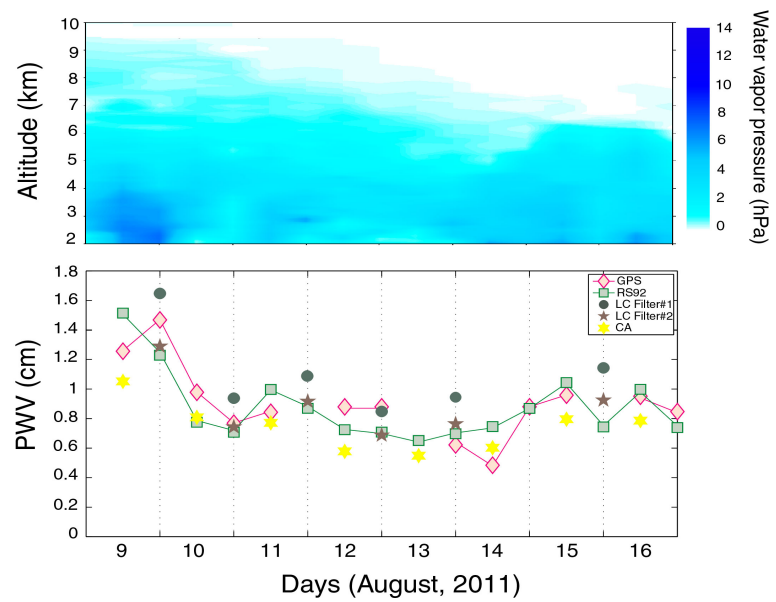
Fig. 5. Daily evolution of PWV (cm) obtained in August at daytime (~ 11:00 UTC) and nighttime (~ 23:00 UTC) using CA and LC, as well as GPS and RS92. In the upper panel is presented the vertical daily evolution of water vapor pressure (hPa) during this period obtained from radiosonde data.

Column water vapor determination in night period

A. Barreto et al.

Title Page

Abstract | Introduction

Conclusions | References

Tables | Figures

◄ | ►

◄ | ►

Back | Close

Full Screen / Esc

Printer-friendly Version

Interactive Discussion